Research article

Elham Heidari, Hamed Dalir*, Moustafa Ahmed, Volker J. Sorger and Ray T. Chen

Hexagonal transverse-coupled-cavity VCSEL redefining the high-speed lasers

https://doi.org/10.1515/nanoph-2020-0437
Received July 30, 2020; accepted September 28, 2020;
published online October 14, 2020

Abstract: Vertical-cavity surface-emitting lasers (VCSELs) have emerged as a vital approach for realizing energy-efficient and high-speed optical interconnects in the data centers and supercomputers. Indeed, VCSELs are the most suitable mass production lasers in terms of cost-effectiveness and reliability. However, there are still key challenges that prevent achieving modulation speeds beyond 30s GHz. Here, we propose a novel VCSEL design of a hexagonal transverse-coupled-cavity adiabatically coupled through a central cavity. Following this scheme, we show a prototype demonstrating a 3-dB roll-off modulation bandwidth of 45 GHz, which is five times greater than a conventional VCSEL fabricated on the same epiwafer structure. This design harnesses the Vernier effect to increase the laser's aperture and therefore is capable of maintaining single-mode operation of the laser for high injection currents, hence extending the dynamic roll-off point and offering increases power output. Simultaneously, extending both the laser modulation speed and output power for this heavily deployed class of lasers opens up new opportunities and fields of use ranging from data-comm to sensing, automotive, and photonic artificial intelligence systems.

Keywords: adiabatic coupling; hexagonal VCSEL; lateral integration.

***Corresponding author: Hamed Dalir**, Omega Optics, Inc., 8500 Shoal Creek Blvd., Bldg. 4, Suite 200, Austin, Texas 78757, USA, E-mail: hamed.dalir@omegaoptics.com. https://orcid.org/0000-0002-9998-3830
Elham Heidari and Ray T. Chen, Microelectronics Research Center, Electrical and Computer Engineering Department, University of Texas at Austin, Austin, Texas 78758, USA
Moustafa Ahmed, Department of Physics, Faculty of Science, King Abdul-Aziz University, 80203 Jeddah 21589, Saudi Arabia
Volker J. Sorger, Department of Electrical and Computer Engineering, George Washington University, Washington, DC 20052, USA

1 Introduction

Semiconductor lasers, allowing for indispensable science and a wide range of technologies, have become one of the most important enablers of photonics-based technologies [1]. Vertical-cavity surface-emitting lasers (VCSEL), a vital class of semiconductor lasers [2], specifically, are gaining importance given their form factor and optoelectronic performance for their use as an optical source in high-speed, short-wavelength communications [3, 4] and sensors [4–6]. For instance, in recent years VCSELs have been deployed aside semiconductor diode lasers as the sources in cost-effective fiber links and data center networks [7–9]. This is due to their distinct features, such as high reliability, low cost and high manufacturing yield, low power consumption, seamless packaging, low lasing threshold and operating currents, high-temperature stability, and straightforward fabrication of dense arrays [4, 10, 11]. For data-transmission applications, a high modulation bandwidth is desired. The 3-dB bandwidth of the VCSEL is limited by thermal effects, parasitic resistance, capacitance, and nonlinear gain effects (such as relaxation oscillations) [12, 13]. Thus, with an appropriate design of the active region and RC parasitics, which bypasses the modulation current outside the active region at high frequencies, a high modulation bandwidth can be attained. Optical feedback has proven to increase the modulation bandwidth of VCSELs, owing to an induced photon–photon resonance (PPR) effect [14–17]. For example, Dalir et al. [18, 19] demonstrated modulation bandwidth enhancement of a VCSEL by adding a single transverse-coupled cavity (TCC) to a primary VCSEL cavity. The underlying principle is to control the delay time in the TCC via an induced slow-light feedback section. However, strong PPR effects suffer comparatively large "kinks" in the light-versus-current (L–I) characteristics indicative of induced laser instabilities due to increased supply currents [18–22]. Nonetheless, multiple TCCs (MTCCs) are advantageous to avoid these instabilities in the linear region of the L–I curve. Indeed, this is the common issue in standard (twin) coupled cavities [18, 23–26] in addition to challenges with respect to optical injection locking [27].

Open Access. © 2020 Elham Heidari et al., published by De Gruyter. This work is licensed under the Creative Commons Attribution 4.0 International License.

In this article, we introduce and demonstrate a new design of a VCSEL combining MTCCs, which aims to enhance slow-light optical feedback, thus extending the temporal laser bandwidth (speed) beyond the limit of the relaxation oscillation frequency. In our design, we propose and show that a VCSEL cavity surrounded by MTCCs adiabatically provides direct slow-light feedback from each TCC to the main lasing cavity. Therefore, even if the direct feedback from each cavity is only moderate, it will yet redistribute the optical field density by funneling the slow-light mode into the central cavity, which effectively allows generating sufficient feedback to extend the temporal laser bandwidth (speed). Following this coupled cavity scheme, we show a resulting modulation bandwidth in the 100 GHz range. We validate this novel laser design paradigm by demonstrating a VCSEL design following a hexagonal multi-cavity approach showing a bandwidth of about 45 GHz, which is an about five times improvement over 'conventional' VCSEL designs realized on the same wafer. Beyond speed performance, the MTCC paradigm can further be used to increase the laser power output; to achieve high-power at single-mode operation, the Vernier effect in the hexagonal VCSEL can be used to form a wider laser aperture [28, 29]. Following this design concept, we demonstrate single-mode operation with a high (>30 dB) side-mode suppression (SMSR) and prominent (>45 dB) signal-to-noise ratio (SNR). Finally, optimizing the lattice design, we show extending the laser stability for higher output power by about three times compared with conventional VCSEL fabricated on same epiwafer [30].

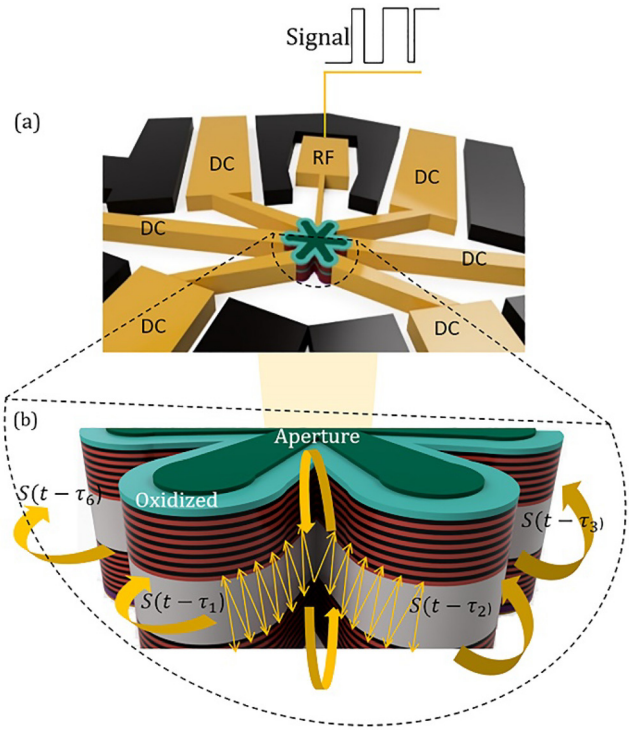

Figure 1: Schematic structure of our hexagonal transverse-coupled-cavity vertical-cavity surface-emitting lasers (VCSEL) (a) Top view, and (b) Cross-sectional view. The six outer cavities are designed to have the same resonant wavelength ω at $I_{\text{feedback}} < I_{\text{th}}$. $I_{\text{laser}} = mI_{\text{th}}$. When I_{laser} increases resonant wavelength red shift like its conventional VCSEL.

2 Structure and concept

The MTCC VCSEL is designed to promote adiabatic light energy sharing between the coupled cavities relative to the central laser cavity (Figure 1). Even if the feedback strength of each cavity is in a moderate range (~0.1 THz) [31], because of its adiabatic design, the laser cavity parametrically accumulates an increased amount of the slow-light portion of the light gain and makes this available for the to-be-modulated cavity. Creating a functional space separation between selective gain and modulation functions is the key to simultaneously achieving high speed and high power in single-mode operation. Furthermore, this design is advantageous by avoiding the optical loss accumulated in the chain of cascaded TCCs [30].

Unlike a conventional VCSEL design, light generated in the MTCC-based laser has an additional lateral component with an angle close to 90° near the cutoff condition of light propagation [32]. Therefore, most of the slow-light effect is reflected at the far end of each feedback cavity and, thence, coupled back into the modulation cavity with a coupling ratio of η. The period of each round trip in the TCC of width L_C is $\tau = \frac{2n_g L_C}{c}$, where c is the speed of light and $n_g = fn$ is the group index with n and f being the average material refractive index and slow-light factor, respectively [18]. If we consider multiple round trips of such coupled slow light inside such a MTCC-based VCSEL, the laser threshold gain G_{thD} can be modified by [33]

$$G_{th} = G_{thD} - \frac{v_g}{W} \ln \prod_{m=1}^{M} |U_m(t-\tau_m)| \tag{1}$$

which constitutes a generalized form for the gain derived in references [33, 34]. Here,

$$U_m(t-\tau_m) = |U_m(t-\tau_m)| e^{j\varphi_m} = 1 + \frac{\eta_m}{\eta_m - 1} \sum_p \sqrt{1-\eta_m^p} e^{-2p\alpha_{cm}L_{cm}} e^{-j2p\beta_{cm}L_{cm}} \sqrt{\frac{S(t-p\tau_m)}{S(t)}} e^{j\theta(t-p\tau_m)-j\theta(t)} \tag{2}$$

where the summation accounts for multiple round trips in the TCC, while $e^{-2p\alpha_{cm}L_{cm}}$ and $e^{-j2p\beta_{cm}L_{cm}}$ are the loss and phase delay, respectively, of slow light during each round trip.

Furthermore, $\alpha_{cm} = f\alpha_m$ and $\beta_{cm} = 2\pi n/(\lambda f)$ are the lateral optical loss and propagation constant, respectively, where α_m is the material loss related to the mth TCC and λ is emission wavelength. For our MTCC case, η_m is the coupling ratio of the slow-light feedback from the mth cavity, while L_{cm} and τ_m are the corresponding length and round-trip time, respectively. Note, $\theta(t - p\tau_m) - \theta(t)$ represents the deviation in the optical phase due to chirping in the mth cavity.

The rate equations of this MTCC VCSEL is given for the injected electron density $N(t)$, photon density $S(t)$ contained in the lasing mode and the optical phase $\theta(t) = \arg[E(t)]$ as

$$\frac{dN}{dt} = \frac{\eta_i}{e} I - \alpha v_g \frac{(N - N_T)}{1 + \varepsilon S} S - \frac{N}{\tau_e} \tag{3}$$

$$\frac{dS}{dt} = \left[\Gamma a v_g \frac{N - N_{th}}{1 + \varepsilon S} - \frac{1}{\tau_p} + \frac{v_g}{W} \sum_{m-1}^{M} \ln|U(t - \tau_m)| \right] S + \Gamma R_{sp} \tag{4}$$

$$\frac{d\theta}{dt} = \frac{\alpha}{2} \left[\Gamma a v_g (N - N_{th}) + \frac{v_g}{W} \sum_{m=1}^{M} \varphi_m \right] \tag{5}$$

where η_i represents the injection efficiency, which is the fraction of terminal current that provides carriers that recombine in the active region, α is the differential gain of the active region whose volume is V, N_T defines the electron numbers at the transparency, and ε is the gain suppression coefficient. Γ and $\tau_p = 1/G_{thD}$ represent the confinement factor and photon lifetime in the lasing cavity, respectively. τ_e is the electron lifetime due to the spontaneous emission rate, R_{sp} is the spontaneous emission rate, and N_{th} is the electron number at the threshold. We solve these rate equations via the 4th order of Runge–Kutta method using sinusoidal current modulation with bias component I_b, modulation component I_m, and modulation frequency f_m. The integration step is set to 0.2 ps. To form the lattice of the 2D VCSEL arrays, six feedback cavities are adiabatically coupled through a star design (Figure 1). These TCCs are assumed identical having a length of $L_{cm} = L_c$ and $\tau_m = \tau$ for slow-light propagation. A typical limitation of the single TCC is the requirement for a strong slow-light coupling into the VCSEL cavity to extend the modulation bandwidth, which demands excessive coupling strengths when modulation frequencies into the mm waveband are desired [33]. Here, we introduce utilizing a MTCC-based design in such a way, as to adiabatically induce a direct slow-light feedback from each TCC. That is, we design the surrounding MTTCs to enable bandwidth enhancement with low and realistically achievable values of the coupling ratio η (Figures 1 and 2).

3 Experimental demonstration of the hexagonal VCSEL

This formulism can predict the MTCC small-signal response as a function of the modulation frequency (Figure 2a); the laser's intensity modulation (IM), including several PPR effects, shows a speed in excess of 40 GHz, which is about

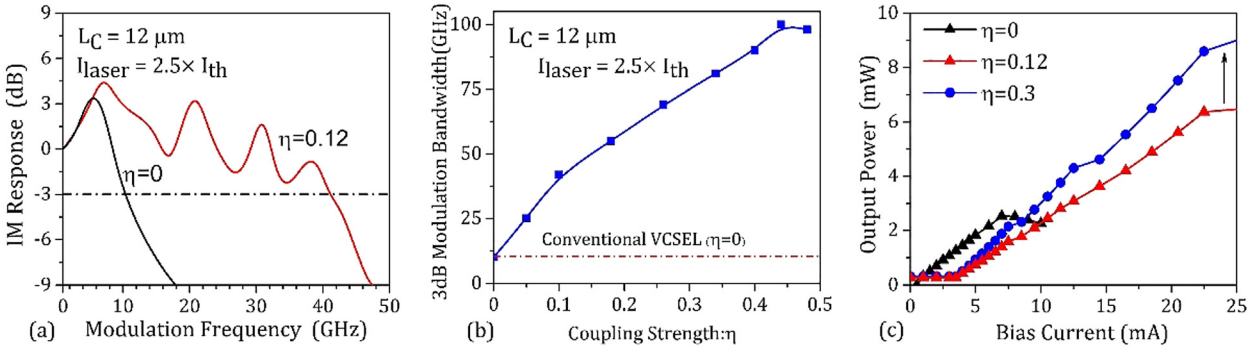

Figure 2: The design of hexagonal transverse-coupled-cavity vertical-cavity surface-emitting lasers (VCSEL).
(a) Small-signal intensity modulation (IM) response for VCSEL with six identical feedback cavities with length and coupling strength of $Lc = 12$ μm and $\eta = 0.12$, respectively. IM response with a robust feedback system ($\eta = 0.12$) provides 3-dB roll-off more than 42 GHz (Equations (1) and (2)). Conventional VCSEL fabricated on the same epiwafer with 3-dB roll-off ~9 GHz is shown for comparison ($\eta = 0$), (b) Shows the 3-dB modulation bandwidth versus coupling strength (η). The 3-dB roll-off can exceed 100 GHz via further increasing the coupling strength to $\eta = 0.45$. Note, the increased of the coupling strength directly affects the stability of the laser, and (c) shows output power as a function of bias current of the inner cavity. The black line with a triangle symbol indicates the L–I curve of a conventional VCSEL with an aperture size of 3×3 μm^2. The red and blue curves are for multiple transverse-coupled-cavity VCSEL (MTCC VCSEL) with six identical feedback cavities and $L_c = 12$ μm. It is noted that linearity of the L–I curve deteriorates as coupling strength increases from $\eta = 0.12$ to 0.3. In addition, there is a trade-off between wall-plug efficiency and kinks in the L–I curve.

fivefold higher than conventional VCSEL design lacking the MTCC approach. In addition, the corresponding response curve shows a high degree of stability; that is, it is relatively robust against changes in the slow-light feedback (η). The IM response of a conventional VCSEL ($\eta = 0$) shows the expected slow (9 GHz) response (Figure 2a) [18, 19, 35]. For a moderate pump and TCC feedback ($I_{laser} = 2.5 \times I_{th} = 8$ mA and $\eta = 0.12$), the IM response exhibits an enhanced carrier to photon resonance (CPR) and multiple PPR before its 3-dB roll-off, which occurs at a bandwidth frequency of 42 GHz (Figure 2a). Increasing the coupling between the inner (modulating) cavity and outer (feedback) cavities exhibit an extended 3-dB roll-off reaching 100 GHz on further increasing the coupling strength to $\eta = 0.45$ (Figure 2b) [36]. Note, that an increased coupling strength, normally, adversely affects the stability of the laser; however, some of these can be accounted for using the added degree of freedom given by the MTCC paradigm. As illustrated in Figure 2c, L–I characteristics start displaying 'kinks' while the coupling strength increases from $\eta = 0.12$ to 0.3.

Figure 3 shows a top view of the fabricated hexagonal VCSEL and the calibrated 45 GHz small-signal measurement test setup. This top emitting VCSEL structure is grown by metal organic chemical vapor deposition on an n^+ substrate. The epitaxial structure consists of 35 pairs of Si-doped bottom $Al_{0.16}Ga_{0.84}As/Al_{0.9}Ga_{0.1}As$ distributed Bragg reflector (DBR), whereas the cavity consists of three 70 Å, $In_{0.3}Ga_{0.7}As$–GaAs quantum wells, and a top 24-period DBR mirror. Inductively coupled plasma etched the mesa into a semiconductor heterostructure, and its etch size was selected to be 2 µm larger than the active diameter (mesa diameter and oxidation time optimization). The aperture mesa diameters used are 3.5 µm wide to ensure single transverse mode operation with a lower threshold current. The inner cavity is an RF-modulated VCSEL with the six identical outer cavities adiabatically coupled to the center cavity, thus providing parametric and selective slow-light feedback. The end interface of each feedback cavity acts as a perfect mirror in the lateral direction, supporting the lateral optical light coupled back into the inner one [37].

However, the TCC-based VCSEL design has two fundamental challenges; (i) a typical limitation of the VCSEL with only a single TCC requires a strong slow-light coupling coefficient to enhance the modulation, and (ii) the TCC(s) add parasitic nonlinearity which reduces the modulation performance [18–21].

To mitigate or entirely avoid both of these limitations, we propose and show that rather than relying on a single cavity, a MTCC design induces direct slow-light feedback

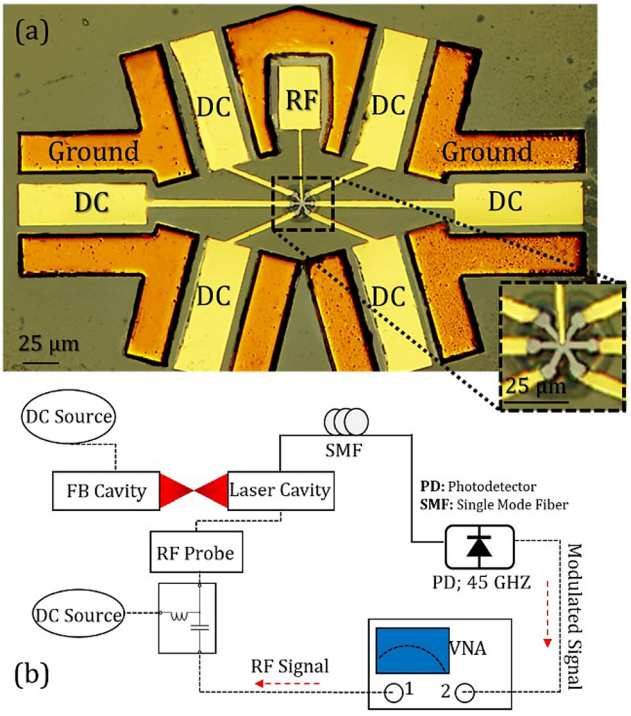

Figure 3: (a) The top-view false optical microscopic image of the fabricated multiple transverse-coupled-cavity vertical-cavity surface-emitting lasers (MTCC VCSEL) with aperture size of 3.5×3.5 µm^2 for inner cavity and six identical feedback, each with a length of 12 µm. With an aim to achieve high-power, single-mode operation, the Vernier effect in lateral integration in a VCSEL can be utilized to form a larger aperture size and hence, more gain medium [28, 29], and (b) our calibrated 45 GHz small-signal measurement setup.

from each TCC, thus enhancing feedback and relaxing coupling coefficient requirements. The small-signal frequency response (S_{21}) of the VCSEL was obtained by generating a low power modulating signal with a vector network analyzer. The output modulated intensity from the inner (laser) cavity with a fixed current is then collected via a single-mode fiber, whereas each of feedback cavities is operated at 2 mA. A high-speed photodetector (PD) collects the VCSEL's RF output and compares it with the original modulating source. The IM response showed enhanced CPR and multiple PPR before its 3-dB roll-off. The 3-dB roll-off of the MTCC-enhanced laser exceeds the conventional design by about fivefold compared with a conventional VCSEL fabricated on the same epiwafer (Figure 4a). While the conventional VCSEL being driven at $I_{conventional} = 7$ mA, which is the maximum power before it saturates, our designed VCSEL is just operated at 8 mA for the inner cavity with surrounding cavities driven at constant current of 2 mA below threshold bias current. Even at this level, our 3-dB roll-off is beyond the PD limit (>45 GHz). Figure 4b

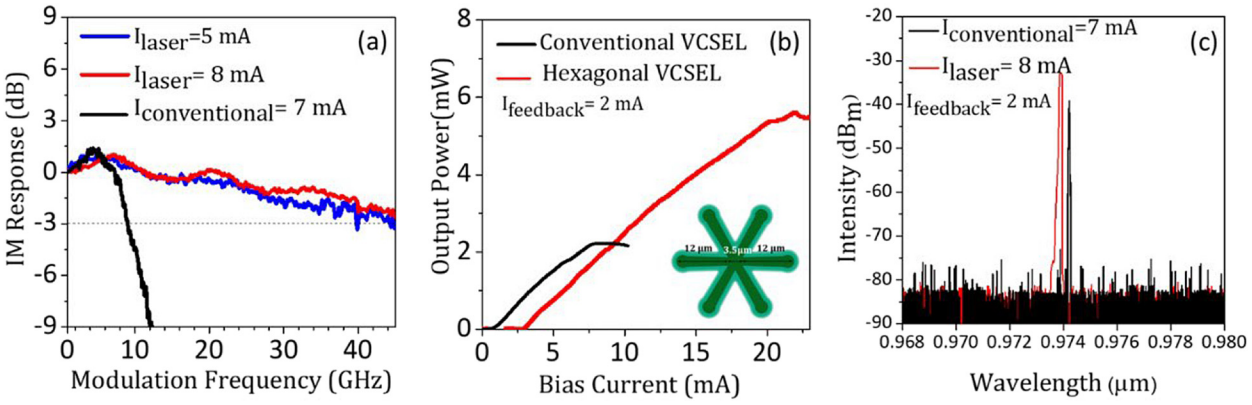

Figure 4: (a) Intensity modulation (IM) response for vertical-cavity surface-emitting lasers (VCSEL) with six identical feedback cavities with the length of L_C = 12 μm and effective aperture size of 3.5 × 25 μm^2. The IM response with a robust feedback system in the hexagonal VCSEL provides a 3-dB roll-off over 45 GHz based on Equations (1) and (2). We project the coupling strength to be η = 0.12. Conventional VCSEL fabricated on the same epi-wafer with 3-dB roll-off ~9 GHz is shown for comparison, (b) shows out-put power for both conventional (black curve) and our hexagonal one (red curve) versus bias current. As seen here, our hexagonal VCSEL can be driven with large of currents (>20 mA) and output power still linearly increases to ~5.5 mW, which is triple of its conventional VCSEL, and (c) a single-mode operation for our hexagonal VCSEL with SMSR of >30 dB and SNR of >45 dB is obtained.

depicts the measured L–I curve for our MTCC VCSEL with an effective aperture size of 3.5 × 25 μm^2, and a conventional VCSEL fabricated on the same epitaxial wafer with an aperture size of 3 × 3 μm^2. Interestingly, this hexagonal VCSEL drives more current even beyond the conventional limitation (>7 mA), the output power linearly increases to about 5.5 mW, which is almost triple that of its conventional counterpart. It is also, important to mention that the threshold current of our hexagonal VCSEL can be further reduced via optimization of the oxide layer structure close to conventional VCSEL. Thanks to the Vernier effect in the MTCC VCSEL, even with such a large oxide aperture, a single-mode operation with SMSR of >30 dB (7 dB higher than a conventional VCSEL design) [38] and SNR of >45 dB are obtained (Figure 4c). Note, that to obtain a coupling of η ~ 0.45 (which potentially provide a 3-dB roll-off ~100 GHz), one can design oxide-free VCSELs recently reported by Deppe [39].

4 Conclusion

In conclusion, we propose a novel design of a 980 nm VCSEL adiabatically and laterally coupled to six hexagonal feedback cavities. Succeeding this approach, we demonstrate a fivefold higher 3-dB roll-off laser modulation bandwidth (>45 GHz limited by the experimental setup) compared with a noncoupled, conventional design.

This coupled hexagonal VCSEL paradigm shows single-mode operation with SMSR > 30 dB, which is 7 dB higher than a conventional VCSEL fabricated on the same epiwafer. Furthermore, with an SNR of >45 dB, the peak output power of 5.5 mW is about triple as high compared with the conventional design. Further bandwidth enhancement for the VCSEL with MTCC is the need for a strong slow-light coupling into the modulating cavity. For example, to obtain η ~ 0.45, it is possible to provide a roll-off of 3 dB–100 GHz. This device concept opens up new opportunities and fields of use ranging from data-comm, to sensing, automotive, and photonic artificial intelligence systems.

Acknowledgments: The authors thank Dr. Gernot Pomrenke, Dr. Luke Graham and Dr. Chung-Yi Su for their fruitful discussions.

Author contribution: All the authors have accepted responsibility for the entire content of this submitted manuscript and approved submission.

Research funding: Air Force Office of Scientific Research (AFSOR) Small Business Innovation Research (SBIR) Program (FA9550-19-C-0003) Naval Research Electronic Warfare Program (N00014-19-1-2595).

Conflict of interest statement: The authors declare no conflicts of interest regarding this article.

References

[1] K. Iga, "Surface-emitting laser-its birth and generation of new optoelectronics field," *IEEE J. Sel. Top. Quant.*, vol. 6, pp. 1201–1215, 2000.

[2] G. de Valicourt, G. Levaufre, Y. Pointurier, et al., "Direct modulation of hybrid-integrated InP/Si transmitters for short and long reach access network," *J. Lightwave Technol.*, vol. 33, pp. 1608–1616, 2015.

[3] S. Kajiya, K. Tsukamoto, and S. Komaki, "Proposal of fiber-optic radio highway networks using CDMA method," *Proceedings of ICUPC '95 – 4th IEEE International Conference on Universal Personal Communications,* Tokyo, Japan, vol. 1995, pp. 496–500, 1996. https://doi.org/10.1109/ICUPC.1995.497058.
[4] K. Iga, "Vertical-cavity surface-emitting laser: it's conception and evolution," *Jpn. J. Appl. Phys.*, vol. 47, pp. 1–10, 2008.
[5] C. P. T. McPolin, J.-S. Bouillard, S. Vilain, et al., "Integrated plasmonic circuitry on a vertical-cavity surface-emitting semiconductor laser platform," *Nat. Commun.*, vol. 7, p. 12409, 2016.
[6] A. Larsson, "Advances in VCSELs for communication and sensing," *IEEE J. Sel. Top. Quant.*, vol. 17, pp. 1552–1567, 2011.
[7] M. Z. Alam, I. D. Leon, and R. W. Boyd, "Large optical nonlinearity of indium tin oxide in its epsilon-near-zero region," *Science*, vol. 352, pp. 795–797, 2016.
[8] R. Rodes, M. R. Rodes, M. Mueller, et al., "High-speed 1550 nm VCSEL data transmission link employing 25 GBd 4-PAM modulation and hard decision forward error correction," *J. Lightwave Technol.*, vol. 31, pp. 689–695, 2013.
[9] C. Choi, L. Lin, Y. Liu, and R. T. Chen, "Performance analysis of 10-μm-thick VCSEL array in fully embedded board level guided-wave optoelectronic interconnects," *J. Lightwave Technol.*, vol. 21, pp. 1531–1535, 2013.
[10] F. Koyama, "Recent advances of VCSEL photonics," *J. Lightwave Technol.*, vol. 24, pp. 4502–4513, 2006.
[11] R. Michalzik, *VCSELs: Fundamentals, Technology and Applications of Vertical-Cavity Surface-Emitting Lasers*, Berlin, Springer, 2012, p. 557–577.
[12] L. A. Coldren, S. W. Corzine, and M. L. Mashanovitch, *Diode Lasers and Photonic Integrated Circuits*, vol. 218, Hoboken, John Wiley & Son, 2012, p. 260.
[13] C. Wilmsen, H. Temkin, and L. A. Coldren, *Vertical-cavity Surface-Emitting Lasers: Design, Fabrication, Characterization, and Applications*, vol. 24, United Kingdom, Cambridge University Press, 2001.
[14] C. Chen and K. D. Choquette, "Analog and digital functionalities of coupled cavity surface emitting lasers," *J. Lightwave Technol.*, vol. 28, pp. 1003–1010, 2010.
[15] A. Paraskevopoulos, H. J. Hensel, W. D. Molzow, et al., in *OFC Conference and the National Fiber Optic Engineers Conference*, paper PDP22, 2006.
[16] P. Westbergh, J. S. Gustavsson, B. Kögel, Å. Haglund, and A. Larsson, "Impact of photon lifetime on high-speed VCSEL performance," *IEEE J. Sel. Top. Quant.*, vol. 17, pp. 1603–1613, 2011.
[17] P. Bardella, W. W. Chow, and I. Montrosset, "Design and analysis of enhanced modulation response in integrated coupled cavities DBR lasers using photon–photon resonance," *Photonics*, vol. 3, p. 4, 2016.
[18] H. Dalir and F. Koyama, "29 GHz directly modulated 980 nm vertical-cavity surface emitting lasers with bow-tie shape transverse coupled cavity," *Appl. Phys. Lett.*, vol. 103, p. 091109, 2013.
[19] H. Dalir and F. Koyama, "High-speed operation of bow-tie-shaped oxide aperture VCSELs with photon–photon resonance," *Appl. Phys. Express*, vol. 7, p. 022102, 2014.
[20] Z. Gao, S. T. M. Fryslie, B. J. Thompson, P. Scott Carney, and K. D. Choquette, "Parity-time symmetry in coherently coupled vertical cavity laser arrays," *Optica*, vol. 4, pp. 323–329, 2017.
[21] S. T. M. Fryslie, M. P. T. Siriani, D. F. Siriani, M. T. Johnson, and K. D. Choquette, "37-GHz modulation via resonance tuning in single-mode coherent vertical-cavity laser arrays," *IEEE Photonics Technol. Lett.*, vol. 27, pp. 415–418, 2015.
[22] Z. Feng, F. Yang, X. Zhang, et al., "Ultra-low noise optical injection locking amplifier with AOM-based coherent detection scheme," *Sci. Rep.*, vol. 8, p. 13135, 2018.
[23] H. Dave, P. Liao, S. T.-M. Fryslie, et al., "Digital modulation of coherently-coupled 2×1 vertical-cavity surface-emitting laser arrays," *IEEE Photonics Technol. Lett.*, vol. 31, pp. 173–176, 2019.
[24] C. Xu, W. E. Hayenga, H. Hodaei, D. N. Christodoulides, M. Khajavikhan, and P. LiKamWa, "Enhanced modulation characteristics in broken symmetric coupled microring lasers," *Opt. Express*, vol. 28, pp. 19608–19616, 2020.
[25] H. Hodaei, M. A. Miri, M. Heinrich, D. N. Christodoulides, and M. Khajavikhan, "Parity-time-symmetric microring lasers," *Science*, vol. 346, pp. 975–978, 2014.
[26] M. A. Miri, P. LiKamWa, and D. N. Christodoulides, "Large area single-mode parity-time-symmetric laser amplifiers," *Opt. Lett.*, vol. 37, pp. 764–766, 2012.
[27] N. Li, H. Susanto, B. R. Cemlyn, I. D. Henning, and M. J. Adams, "Locking bandwidth of two laterally-coupled semiconductor lasers subject to optical injection", *Sci. Rep.*, vol. 8, p. 109, 2018.
[28] M. Li, N. Zhang, K. Wang, J. Li, S. Xiao, and Q. Song, "Inversed Vernier effect based single-mode laser emission in coupled microdisks," *Sci. Rep.*, vol. 5, p. 13682, 2015.
[29] R. Todt, Th. Jacke, R. Laroy, G. Morthier, and M.-C. Amann, "Demonstration of Vernier effect tuning in tunable twin-guide laser diodes," *IEEE Proc. J. Optoelectron.*, vol. 152, pp. 66–71, 2005.
[30] H. R. Ibrahim, M. Ahmed, and F. Koyama, in *24th Microoptics Conference* (MOC), Japan, 2019, pp. 300–301.
[31] E.Heidari, H.Dalir, M.Ahmed, M. H.Teimourpour, V. J.Sorger, and R. T.Chen, in *Proc. SPIE 11286, Optical Interconnects 2020 XX*, p. 112861B.
[32] H. Dalir and F. Koyama, "Bandwidth enhancement of single-mode VCSEL with lateral optical feedback of slow light," *IEICE Electron. Express*, vol. 8, pp. 1075–108, 2011.
[33] M. Ahmed, A. Bakry, M. S. Alghamdi, H. Dalir, and F. Koyama, "Enhancing the modulation bandwidth of VCSELs to the millimeter-waveband using strong transverse slow-light feedback," *Opt. Express*, vol. 23, pp. 15365–15371, 2015.
[34] R. Lang and K. Kobayashi, "External optical feedback effects on semiconductor injection laser properties," *IEEE J. Quant. Electron.*, vol. 16, pp. 347–355, 1980.
[35] X. Gu, M. Nakahama, A. Matsutani, M. Ahmed, A. Bakry, and F. Koyama, "850 nm transverse-coupled-cavity vertical-cavity surface-emitting laser with direct modulation bandwidth of over 30 GHz," *Appl. Phys. Express*, vol. 8, p. 082702, 2015.
[36] K. Iga, in *Proc. SPIE 11263 (VECSELs) X*, 2020, p. 1126302.
[37] H. Dalir, Y. Takahashi, and F. Koyama, "Low-voltage, high-speed and compact electro-absorption modulator laterally integrated with 980-nm VCSEL," *Opt. Express*, vol. 22, pp. 25746–25755, 2014.
[38] K. Iga, F. Koyama, and S. Kinoshita, "Surface emitting semiconductor lasers," *IEEE J. Quant. Electron.*, vol. 24, pp. 1845–1855, 1988.
[39] M. Bayat and D. G. Deppe, "Laser characteristics for VCSELs for 77 K and 4 K optical data applications," *IEEE J. Quant. Electron.*, vol. 56, pp. 1–6, 2020.